Biomaterials 81 (2016) 93–103

Contents lists available at ScienceDirect

Biomaterials

journal homepage: www.elsevier.com/locate/biomaterials

Self-adjuvanted hyaluronate – antigenic peptide conjugate for transdermal treatment of muscular dystrophy

Won Ho Kong [a, 1], Dong Kyung Sung [b, 1], Hyemin Kim [a], Jeong-A Yang [a], Nicholas Ieronimakis [c], Ki Su Kim [d], Jeehun Lee [b], Deok-Ho Kim [c], Seok Hyun Yun [d], Sei Kwang Hahn [a, *]

[a] Department of Materials Science and Engineering, Pohang University of Science and Technology (POSTECH), 77 Cheongam-ro, Nam-gu, Pohang, Kyungbuk, 790-784, Republic of Korea
[b] Department of Pediatrics, Samsung Medical Center, Sungkyunkwan University, School of Medicine, 50 Irwon-dong, Gangnam-gu, Seoul, 135-710, Republic of Korea
[c] Department of Bioengineering, University of Washington, Seattle, WA 98195, USA
[d] Wellman Center for Photomedicine and Harvard Medical School, Massachusetts General Hospital, Cambridge, MA 02139, USA

ARTICLE INFO

Article history:
Received 21 August 2015
Received in revised form
28 November 2015
Accepted 2 December 2015
Available online 15 December 2015

Keywords:
Hyaluronate
Peptide
Conjugate
Transdermal
Vaccine

ABSTRACT

Duchenne's muscular dystrophy (DMD) is a neuromuscular disorder accompanied with muscle weakness and wasting. Since myostatin was reported to be a key regulator of muscle wasting, myostatin inhibitors have been investigated as therapeutic candidates for the treatment of muscular diseases. Here, we report an antigenic peptide of myostatin fragment (MstnF) conjugated to hyaluronate (HA) with a low molecular weight (MW, 17 kDa) for transdermal immunotherapy of DMD. Facilitating the transdermal delivery, the low MW HA showed a boosting effect on the immunization of MstnF possibly by engaging both toll-like receptors and cluster of differentiation 44 (CD44). *In vivo* two-photon microscopy clearly visualized the effective transdermal penetration of HA-MstnF conjugates into deep intact skin layers. The transdermal immunization of *mdx* mice significantly increased antibody titers against myostatin. Furthermore, the *mdx* mice immunized with HA-MstnF conjugates resulted in statistically significant improvement in the biochemical and pathological status of skeletal musculature as well as functional behaviors.

1. Introduction

Duchenne's muscular dystrophy (DMD) is a devastating neuromuscular disease by the mutation of *dystrophin* gene, which causes the loss of dystrophin protein in cardiac and skeletal muscles [1]. The pathophysiology of DMD is characterized by progressive muscle weakness and muscle wasting, leading to the loss of ambulation, hypoventilation, and respiratory failure. Over the past decade, myostatin has emerged as a key negative regulator of skeletal muscle development and a major target for the treatment of muscle wasting diseases like DMD [2]. The knockout of *myostatin* in mice resulted in an increase of skeletal muscle mass and improvement of muscular dystrophy phenotype [1,2]. Accordingly, strategies for myostatin inhibition have been widely investigated including active immunization against myostatin with vaccines [3,4]. Among various immunotherapies [5,6], peptide-based vaccines have been successfully applied to patients with chronic hepatitis C virus infection [7], allergic diseases [8], autoimmune diseases [9], and malignancies [6,10]. In a similar manner, a myostatin fragment (MstnF) antigenic peptide can be developed for the treatment of DMD via active immunization.

The delivery of vaccines is mostly carried out by intramuscular or subcutaneous injection. However, invasive vaccination has several important disadvantages such as needle stick injuries, needle-phobia, and non-compliance especially for children [11]. Substantial progress has been achieved toward alternative needle-free vaccine delivery systems using jet-injection, and respiratory, cutaneous, and transdermal delivery methods [11]. Among them, facile transdermal vaccine delivery seems the most exciting and challenging to target the epidermal keratinocytes and skin resident immunocompetent cells [12]. However, the exploitation of

* Corresponding author.
E-mail address: skhanb@postech.ac.kr (S.K. Hahn).
[1] These authors contributed equally to this work.

http://dx.doi.org/10.1016/j.biomaterials.2015.12.007
0142-9612/

transdermal vaccine delivery has been limited likely due to the extraordinary barrier properties of stratum corneum [13]. As we reported elsewhere [14,15], hyaluronate (HA) can be a key molecule for the transdermal delivery of biomacromolecules. The hygroscopic HA can hydrate skin tissue and facilitate the transdermal delivery. Remarkably, even high molecular weight (MW) HA was also reported to be absorbed from the surface of skin, and pass through stratum corneum and underlying skin layers including epidermis, dermis, and lymphatic endothelium [16]. These results suggest that drugs conjugated to HA in the forms of chemical drugs, peptides or proteins can be delivered as far as the deep layers of dermis and dermal cells having HA receptors [17].

Moreover, low MW HA fragment was known to act as an endogenous danger signal by triggering the transduction pathway of toll-like receptor 2 (TLR2) and TLR4 in immunocompetent cells [18,19]. HA in the extracellular matrix (ECM) has a high molecular weight, but undergoes intensive metabolic breakdown and consequent accumulation of fragmented low MW HA at the neoplastic or inflammatory sites [19]. The HA fragment can activate immunocompetent cells, such as keratinocytes, Langerhans cells (LCs), dendritic cells (DCs), and T lymphocytes. HA fragments also stimulate the production of chemokines and cytokines, and increase self-defense of the skin by inducing β-defensin 2 via TLRs [20,21]. These aspects reflect the possibility of HA as a promising vaccine adjuvant, as well as a facile transdermal delivery carrier [17].

In this work, we developed a self-adjuvanted HA-MstnF conjugate for transdermal active immunization against myostatin, evoking immunomodulatory activity possibly through TLR mediated activation of skin resident immune cells. *In vivo* two-photon microscopy was carried out to visualize the transdermal penetration of HA-MstnF conjugates into deep intact skin layers. After that, we examined transdermal delivery of HA-MstnF conjugates for the non-invasive immunization against myostatin in the *mdx* mouse model of DMD [22]. We evaluated the amelioration of dystrophic phenotypes such as body weight change, functional behavior, antibody formation, serum creatine phosphokinase (CPK) activity, and size distribution of muscle fibers in the transdermally immunized *mdx* mice with histological analysis. These findings are discussed for further design and development of transdermal therapeutic vaccines.

2. Materials and methods

2.1. Synthesis of HA-MstnF conjugate

To prevent endotoxin contamination, a series of low MW HA samples (MWs of 5, 17, 100, and 200 kDa, Lifecore Biomedical) with a very low endotoxin content less than 0.01 EU/mg were used in all experiments. HA derivative carrying aldehyde (HA-ALD) was prepared as we described elsewhere [14]. Briefly, 1.0 g of HA with a MW of 17 kDa was dissolved in 100 mL of triple-distilled water. Sodium periodate ($NaIO_4$) was added to the HA solution at 1.0 M ratio of HA repeating unit. After reaction in dark for 3 h, excess amount of ethylene glycol ($HOCH_2CH_2OH$, 1 g) was added to terminate the reaction. The resulting solution was dialyzed against distilled water and then lyophilized for 3 days. The substitution ratio of aldehyde in HA-ALD was analyzed by ^{1}H NMR (DPX500, Bruker). After that, HA-MstnF conjugate and HA - scrambled (scr) MstnF conjugate were synthesized by the coupling reaction of HA-ALD with amine groups of MstnF (V FLQ KYP HTH LVH QA, Peptron) and scrambled MstnF (T FHQ VLQ HKV APY LH, Peptron) at pH 5 in the presence of 5 M excess of sodium cyanoborohydride ($NaBH_3CN$). The peptide content in the conjugate was determined by Bradford assay and GPC analysis. The transdermal delivery and the cellular uptake of HA-MstnF conjugate were visualized using fluorescein isothiocyanate (FITC)-labeled MstnF peptide (Peptron). To analyze the conjugation site of the MstnF peptide to HA-ALD, HA-MstnF conjugate was dissolved in Tris buffer (100 mM Tris–HCl, pH 8.0) containing 10 mM $CaCl_2$. The HA-MstnF conjugate solution was incubated with α-chymotrypsin from bovine pancreas (Sigma) at an α-chymotrypsin/MstnF peptide ratio of 1/20 (w/w) at room temperature for a day. The resulting solution was purified by centrifugal filtration (MWCO = 3 kDa) to remove degraded peptide fragments and the purified product was analyzed by ^{1}H NMR.

2.2. JAWS II cell culture

JAWS II cell, a granulocyte-macrophage colony-stimulating factor (GM-CSF) dependent mouse DC line, was purchased from ATCC. Cells were grown in α-minimum essential medium (α-MEM, Gibco) supplemented with 1 mM sodium pyruvate, 5 ng/mL murine GM-CSF (R&D Systems), and 20% fetal bovine serum (FBS, Gibco) under a humidified 5% CO_2 atmosphere at 37 °C. Cell cultures were maintained by transferring non-adherent cells to a centrifugal tube and treating attached cells with 0.25% trypsin and 0.03% EDTA at 37 °C for 5 min after washing with phosphate buffered saline (PBS, Gibco). The two cell populations were pooled together and dispensed into new culture flasks.

2.3. In vitro DC activation and flow cytometry

Phenotypes of DC lines were analyzed by fluorescence-activated cell sorting (FACS, BD Biosciences). JAWS II cells were incubated with a predetermined amount (60 μM) of samples for 48 h and harvested by trypsinization. After washing with FACS buffer (2% fetal calf serum, FCS and 0.1% NaN_3 in PBS), the cells were blocked with anti-mouse CD16/CD32 on ice for 15 min, followed by washing and then dispensing 2×10^5 cells in 50 μL of FACS buffer into each well of 96-well plate. The cells were stained on ice for 30 min using FITC-conjugated anti-mouse, CD80, CD86, major histocompatibility complex (MHC) I, and MHC II at 0.5 μg per well. After washing with a FACS buffer containing propidium iodide (PI) to stain dead cells once, each sample was resuspended in 0.2 mL of PBS and subjected to the analysis of FACS. Lipopolysaccharide (LPS, 50 ng/mL) was used as a positive control.

2.4. In vitro DC activation and cytokine analysis

To evaluate proinflammatory cytokine expression, cells were added into each well of 6-well culture plate at a cell density of 1×10^6 cells/mL and grown in complete culture medium for 24 h. The medium in the wells were then replaced with fresh complete culture medium containing 60 μM of four HA samples with a different MW and incubated for 48 h. The MW of HA was 5, 17, 100, and 200 kDa, respectively. The MW of HA in HA-MstnF conjugate was 17 kDa. LPS (50 ng/mL) was used as a positive control. After incubation, the supernatant was collected by centrifugation at 400 × g for 10 min and stored at −80 °C before use. The expression of pro-inflammatory cytokines such as interleukin (IL)-1β, IL-6, IL-12, and tissue necrosis factor (TNF)-α was assessed by enzyme-linked immunosorbent assay (ELISA) according to the manufacturer's protocol (R&D Systems).

2.5. Animal maintenance

C57BL/10ScSn-Dmdmdx/J (*mdx*) mice were originally purchased from the Jackson laboratory. All animals were used following guidelines set forth by the American Association for Accreditation of Laboratory Animal Care (AAALAC). All animal experiments were

reviewed and approved by the Institutional Animal Care and Use Committee (IACUC) of Samsung Biomedical Research Institute (SBRI). Individual body weights of all animals were measured weekly. One day before the transdermal immunization, the fur on the abdominal skin was removed by the application of hair removal cream (Veet). The skin was gently wiped with damp cloth, finished up by a couple of rinses with distilled water, and carefully dried. After termination of the study, the animals were sacrificed by cardiac puncture under isoflurane anesthesia for biochemical and histopathological examination.

2.6. In vivo two-photon microscopy

In vivo two-photon fluorescence microscopy and *ex vivo* conventional confocal microscopy were performed to visualize the deep penetration of HA-MstnF conjugate through the epidermis and dermis. Eight weeks old *mdx* mice (male, n = 5) were anesthetized with isoflurane and topically treated with 180 μL of HA-MstnF conjugate or control samples on a skin surface (1 cm × 1 cm) at a dose of 0.5 mg peptide/head. After careful drying, the skin was gently wiped with a damp cloth, finished up by a couple of rinses with distilled water, and dried. At 6 h post-treatment, the animals were anesthetized with ketamine and xylazine (100 mg/kg and 10 mg/kg) via intraperitoneal injection, and subjected to the two-photon fluorescence microscopy (TCS SP5II MP SMD, Leica). Two-photon excitation fluorescence signal of FITC and second harmonic generation signal of collagen structure were obtained using a titanium-sapphire laser at the wavelength of 940 nm for FITC and collagen. Images were collected as Z-stacks (xyz, 400 Hz) using 512 × 512 pixels and analyzed with LAS AF Lite (Leica) and Image J software (National Institute of Health). After termination of the study, animals were sacrificed with a lethal dose of pentobarbital. Dissected skin sample was fixed, embedded in optimal cutting temperature (OCT) compound, and cryosectioned. Tissue sections were analyzed with a confocal microscope (LSM 510, Carl Zeiss).

2.7. Transdermal immunization

Eight weeks old *mdx* mice (male, n = 10) were anesthetized with isoflurane and topically treated with 180 μL of HA-MstnF conjugate or control samples on the surface of abdominal skins at a dose of 0.5 mg peptide per head. Booster doses were administrated at the same dose one week post-primary immunization. After termination of the study, the animals were sacrificed under general anesthesia with ketamine (0.5 mg/kg via intraperitoneal injection) and subjected to biochemical and histopathological analyses.

2.8. Behavior tests

A rotarod test (Columbus Instruments) was performed to assess motor functions once a week (same day and time of each week) according to the previously described protocol [1]. Briefly, mice were placed on the stationary rods that were gradually brought to a constant speed of 20 rpm. The latency to fall was recorded as a maximum time on the rod. Three trials with a 15 min rest between trials per mouse per session were recorded and averaged. Mice were acclimated for 2 weeks before the first data collection.

2.9. Evaluation of immune responses

Blood samples were collected through a cardiac puncture. Serum was separated by centrifugation at 600 × g for 10 min and stored at −80 °C until use. Serum CPK activities were measured with an automatic biochemical analyzer (DRI-CHEM, Fujifilm). Following cardiac perfusion, gastrocnemius and diaphragm muscles were collected and fixed in 10% neutral-buffered formalin solution for 3 days. The fixed tissues were embedded in paraffin and 4 μm thick tissue sections were stained with hematoxylin and eosin (H&E) and Masson's trichrome. All images were taken under a light microscope (Nikon) at × 400 magnification. Morphometric measurement and analysis were performed digitally using Image J software. Fibrosis was quantified as a percentage of area stained with Masson's trichrome using Image J software. Sircol collagen assay kits (Biocolor Assays) were used to measure total collagen contents in the cryo-conserved gastrocnemius muscle samples.

2.10. Antibody titration

All sera samples were individually processed and myostatin specific IgG antibody levels were determined quantitatively by ELISA. Briefly, recombinant myostatin (R&D Systems) was diluted

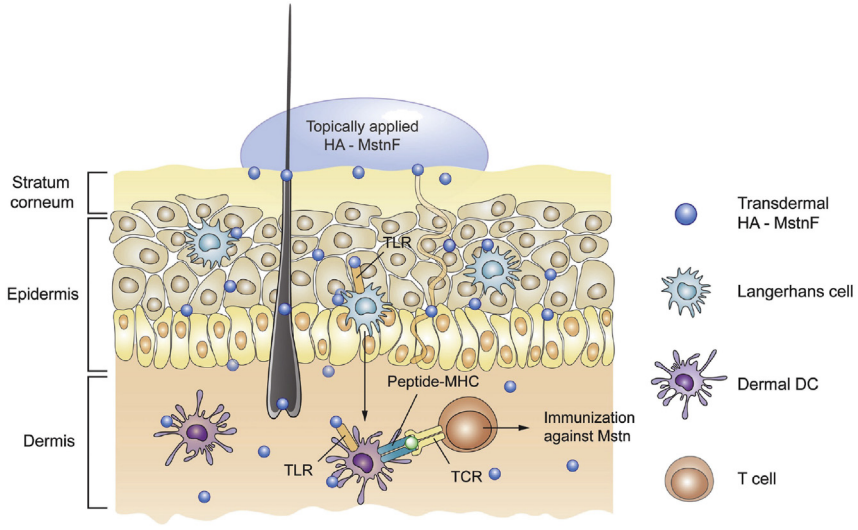

Fig. 1. Schematic illustration for the transdermal delivery of self-adjuvanted hyaluronate (HA) - antigenic peptide (myostatin fragment, MstnF) conjugate and the following immunization against myostatin.

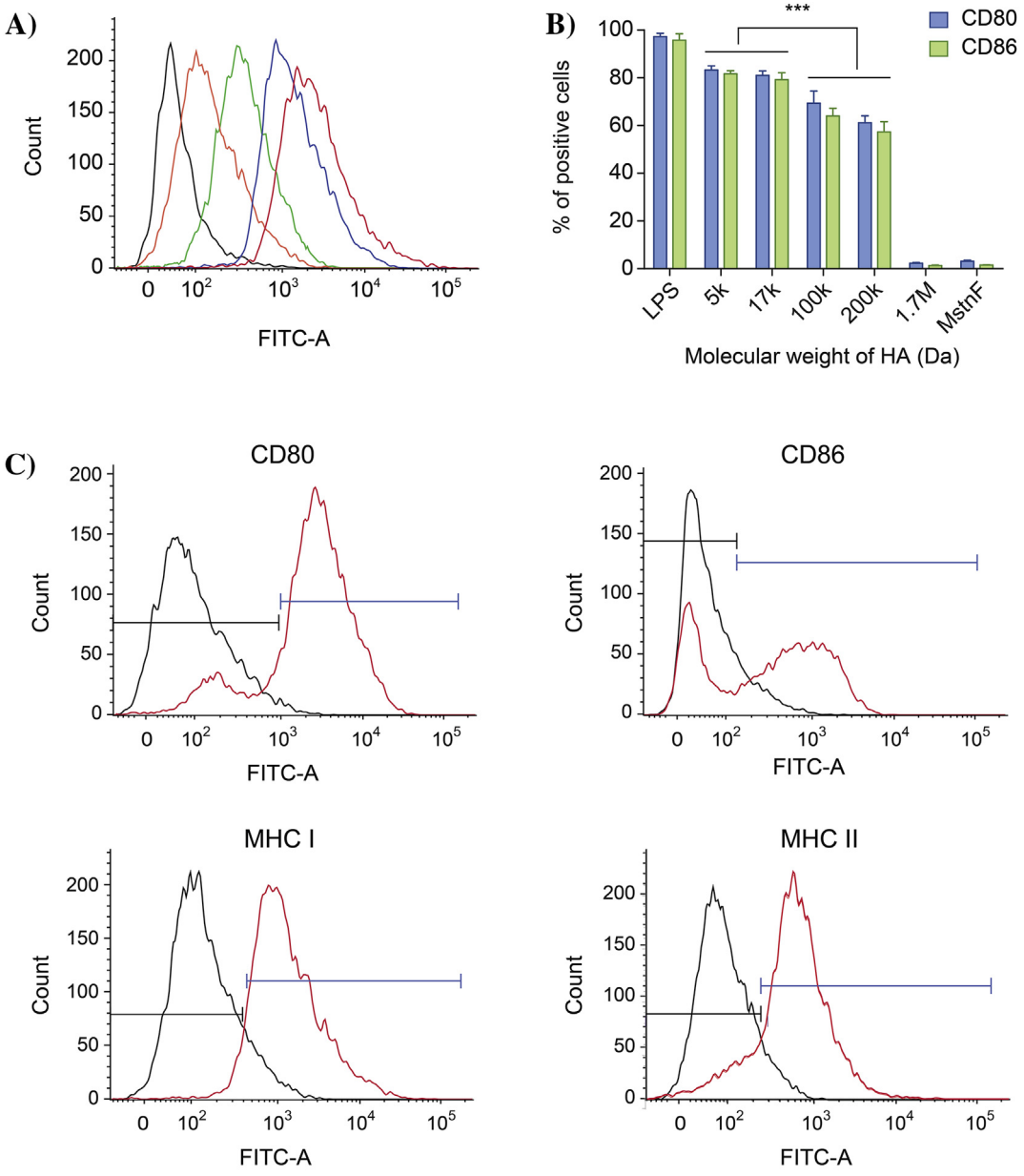

D)

MW (kDa)	The percentage of JAWS II cells positive for maturation markers			
	CD80	CD86	MHC I	MHC II
5	82.3 ± 3.3	80.8 ± 4.9		80.1 ± 4.9
17	80.1 ± 4.2	78.3 ± 3.7	93.3 ± 4.5	72.3 ± 3.5
100	68.4 ± 4.6	63.1 ± 5.1		69.1 ± 2.4
200	60.3 ± 5.2	55.4 ± 5.2		57.2 ± 1.8

Fig. 2. (A) Effect of HA molecular weight (MW) on the internalization of antigenic peptide into a mouse dendritic cell (DC) line of JAWS II cells. The black histogram in panel represents the control of untreated cells. The cells were incubated with MstnF-FITC for 24 h (orange line) or HA-MstnF-FITC conjugates for 24 h (blue line) and 48 h (red line) prior to trypsinization for FACS analysis. The competitive binding test was performed after preincubation with 6.0 μM of HA (MW = 1.7 MDa) for 2 h prior to incubation with HA-MstnF-FITC conjugates for 24 h (green line). (B) The maturation of JAWS II cells in response to the treatment with various MW HAs. The expression of CD80 and CD86 was analyzed by flow cytometry of three independent experiments. (C) Representative histogram for the matured surface marker expression after stimulation of JAWS II cells with low MW HA (17 kDa). The black histogram in each panel represents staining of untreated JAWS II cells with the corresponding antibody. (D) The percentage of JAWS II cells expressing the surface maturation markers from pooled data of three independent experiments. (For interpretation of the references to colour in this figure legend, the reader is referred to the web version of this article.)

to 1.0 mg/mL in 50 mM carbonate buffer (pH 9.6) and then 100 μL of the solution was added to each well of 96 well polystyrene plate (Nunc) for incubation at 4 °C overnight. After washing five times with PBS containing 0.05% Tween-20 (PBS-T), each well of the plate was added with 100 μL of a 100 dilution of serum sample (in PBS contacting 1% BSA) and incubated at room temperature for 1 h. The plate was then washed with PBS-T five times. Subsequently, 100 μL of a 1000 dilution (in PBS contacting 1% BSA) of horseradish peroxidase (HRP)-labeled rabbit anti moues IgG was added to each well, which was incubated at 37 °C for several min until color appeared. The reaction was stopped by adding 50 μL of HCL (1 M) to each well and optical density (OD) at 450 nm was measured with a micro-plate reader. The binding affinity of the antigen specific IgGs from mice sera was assessed by Western blot analysis. Briefly, recombinant murine myostatin protein (800 ng) or BSA (300 ng) was loaded onto sodium dodecyl sulfate (SDS) polyacrylamide gels, subjected to electrophoresis, and then transferred onto nitrocellulose (NC) membrane. Each membrane was incubated with pooled sera (dilution, 1:100) from each group. Following 1 h incubation with appropriate pooled sera, membranes were rinsed with PBS-T thrice. Specifically bound antibody was detected by incubating membranes with HRP conjugated rabbit anti-mouse IgG (dilution, 1:1000). The blotting conditions were identical for all membranes.

2.11. Statistical analysis

Data are expressed as means ± standard deviation from several animals in a group in a few separate experiments. The statistical significance of the differences was calculated by unpaired Student's *t*-test and one-way ANOVA. For statistical designations in figures, * denotes $P < 0.05$, ** denotes $P < 0.01$, *** denotes $P < 0.001$, and **** denotes $P < 0.0001$. Unless stated, independent experiments were run at least in triplicate.

3. Results and discussion

3.1. Synthesis and characterization of HA-MstnF conjugate

As schematically shown in Fig. 1, we developed a facile transdermal immunization system using HA-antigenic peptide conjugates. HA can facilitate the penetration of antigenic peptides through the skin and function as a self-adjuvant for effective transdermal immunization. Low MW HA can bind dermal DCs and epidermal LCs through HA receptors and TLRs (Fig. 1). The low MW HA has adjuvant effect via the TLR signaling pathway, providing an ideal milieu of immune modulation. As a model antigenic peptide, MstnF was conjugated to HA by the coupling reaction between amine groups of peptide and aldehyde (ALD) groups of low MW HA-ALD (Fig. S1). At an acidic condition of pH 5, aldehyde groups can preferably react with N-terminal amine groups of peptide due to the pK_a difference between N-terminal amine groups (*ca.* 8) and amine groups of lysine (*ca.* 10) [14,16].

To analyze the conjugation site of MstnF peptide to HA-ALD, ^1H NMR analysis was carried out after digestion with α-chymotrypsin. The α-chymotrypsin is a serine endoproteinase which specifically cleaves peptide bonds at the C-termini of Y, F and W. Because the

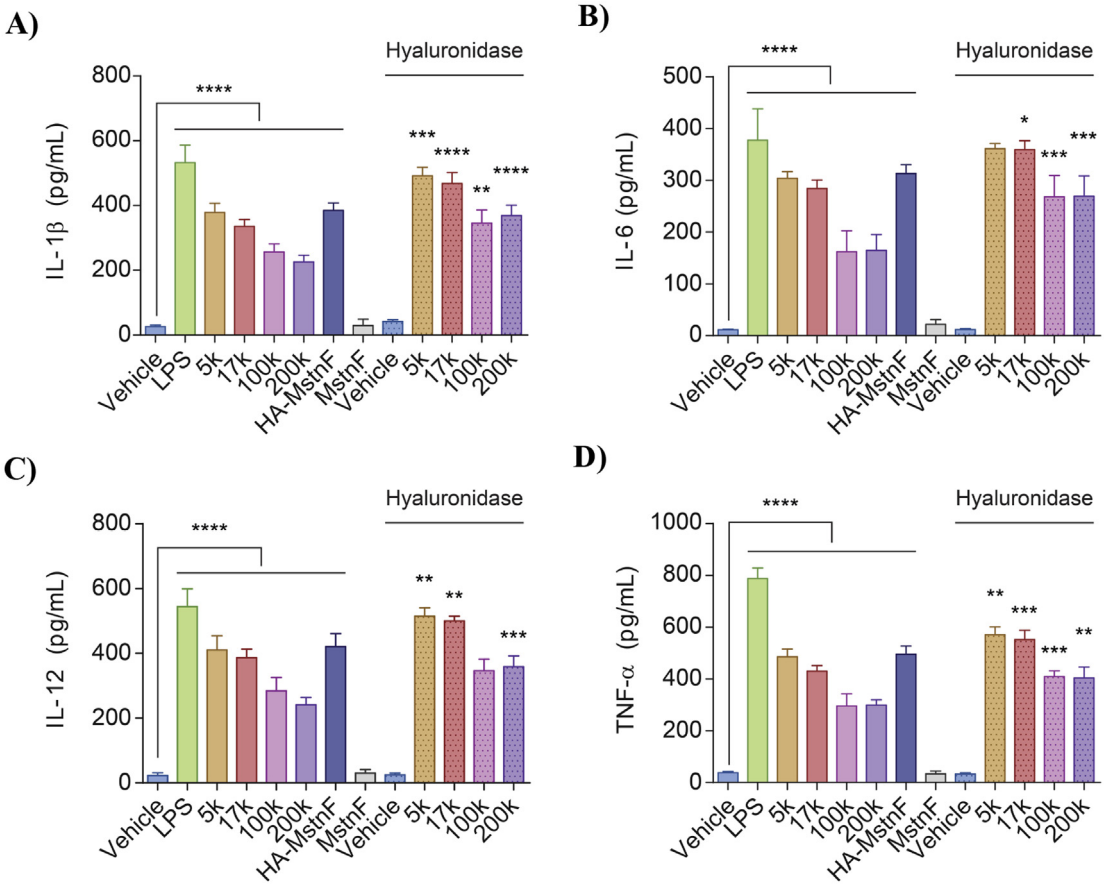

Fig. 3. Effect of various MW HAs on the production of proinflammatory cytokines: (A) interleukin (IL)-1β, (B) IL-6, (C) IL-12, and (D) TNF-α in the culture supernatant of JAWS II cells. The results represent cytokine secretion from three independent experiments.

amino acid sequence of MstnF is V FLQ KYP HTH LVH QA, it can be degraded to three fragments, VF, LQ KY, and P HTH LVH QA. After digestion and purification, C-2 proton (α) peak of three histidines at 8.58 ppm disappeared (Fig. S2), reflecting that P HTH LVH QA fragments without the conjugation site to HA-ALD were removed by centrifugal filtration. On the basis of the results, we assumed that the enzymatic digestion of peptides was almost 100%. The β peaks at δ = 7.24–7.26 correspond to 5 protons at aromatic rings of phenylalanine, and the γ and δ peaks at δ = 7.04 and 6.75 correspond to 4 protons at aromatic rings of tyrosine (Fig. S2). From the integrated peak areas, 63% of the HA-ALD might react with N-terminal amine groups of the MstnF peptide and 37% of HA-ALD might react with ε-amino groups on the lysine of the peptide. The results clearly reflected more preferred conjugation of HA-ALD to the N-terminal amine group than the lysine of MstnF peptide at low pH due to their pK_a difference.

We hypothesized that the combination of HA and MstnF would elicit host derived neutralizing antibody against myostatin. The amino acid sequence of MstnF (V FLQ KYP HTH LVH QA) corresponds to the sequence from 50 to 64 of the mature myostatin. The successful synthesis of HA-MstnF conjugate was also confirmed by GPC analysis (Fig. S3). The retention time of the peptide was shifted after its conjugation to HA. The peptide content in HA-MstnF conjugate was determined from the GPC peak area at 280 nm. The number of peptide molecules per single HA chain in the conjugate could be controlled from 2 to 10 with a bioconjugation efficiency around 90% as determined by GPC and Bradford assay (Fig. S4). The conjugation efficiency gradually decreased from the feeding ratio of 9, likely due to the enhanced steric hindrance at the reaction site. Based on the results, HA-MstnF conjugates prepared by using the feed ratio of 6 were exploited for the following studies.

3.2. Effect of HA MW on in vitro maturation of DCs

DCs are the primary antigen presenting cells (APCs) that initially regulate primary T cell responses and stimulate memory responses to bridge different arms of immune systems [23]. DCs are present in an immature state in the skin until immunological stimuli lead to their rapid maturation. This maturation is accompanied by the elevated expression of co-stimulatory molecules and the production of proinflammatory cytokines for effective T cell activation and migration [23]. The maturation of DCs in adjacent tissue is an important step for effective immune responses. The process of DC maturation is initiated by the internalization of antigens. Hence, the intracellular uptake of HA-MstnF conjugate in the DC line (JAWS II cells) was initially compared with that of a control peptide by FITC-labeling peptides and analyzing their internalization via flow cytometry (Fig. 2A). While JAWS II cells treated with MstnF did not show an obvious peak shift at a concentration up to 10 μg/mL, those treated with HA-MstnF conjugates showed a prominent right peak shift, suggesting enhanced cellular uptake of the conjugate. A competitive binding test with pre-incubation of HA (MW = 1.7 MDa) confirmed the effective cellular internalization of

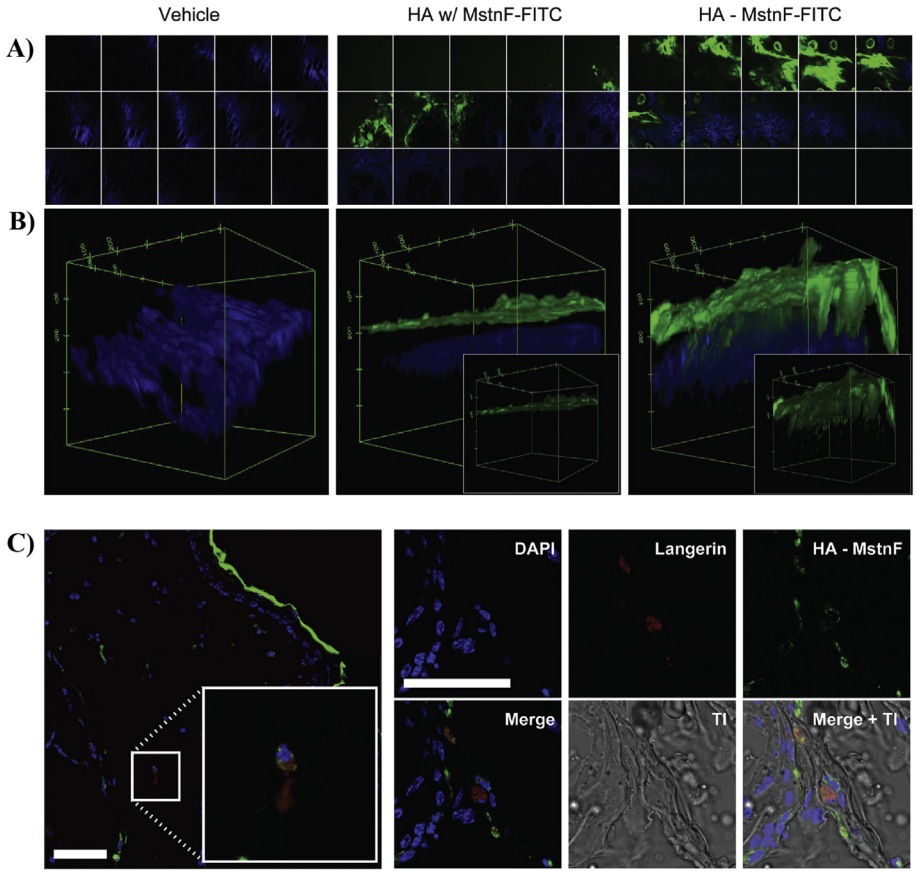

Fig. 4. *In vivo* two-photon microscopic (A) cross-sectional views (246 μm in length) and (B) 3-dimensional projection of intact mouse skin treated with either the control of vehicle or HA-MstnF-FITC conjugate in green (inset). The blue fluorescence represents collagen fibers (n = 3). (C) *Ex vivo* confocal microscopic images after labeling transdermal HA-MstnF conjugate with FITC and immnohistochemical staining of langerin in Langerhans cells (scale bar = 50 μm). (For interpretation of the references to colour in this figure legend, the reader is referred to the web version of this article.)

HA-MstnF conjugate into JAWS II cells via HA receptor-mediated endocytosis [15,16].

Consecutively, we examined the effect of the HA MW on DC maturation in immature JAWS II cells (Fig. 2B). Cells were exposed to 60 μM of HA with a MW of 5, 17, 100 or 200 kDa for 48 h and assessed by flow cytometry for mature DC surface markers of CD80 and CD86 [24]. DCs treated with high MW HA (1.7 MDa) or MstnF peptide were also analyzed as further controls for the effect of HA on cytokine induction. HA with a MW of 100 or 200 kDa induced low-to-moderate levels of DC maturation, but HA with a MW of 5 or 17 kDa induced obvious DC maturation (Fig. 2B). The effect of HA with a MW of 17 kDa was also observed on additional markers of MHC I and MHC II [25], reflecting DC maturity (Fig. 2C and D). In contrast, HA with a MW of 1.7 MDa or MstnF peptide did not induce any significant expression of these maturation markers.

We further investigated the effect of HA MW on DC maturation by evaluating their secretion of proinflammatory cytokines [26]. JAWS II cells were stimulated with various MW HAs for 48 h and the

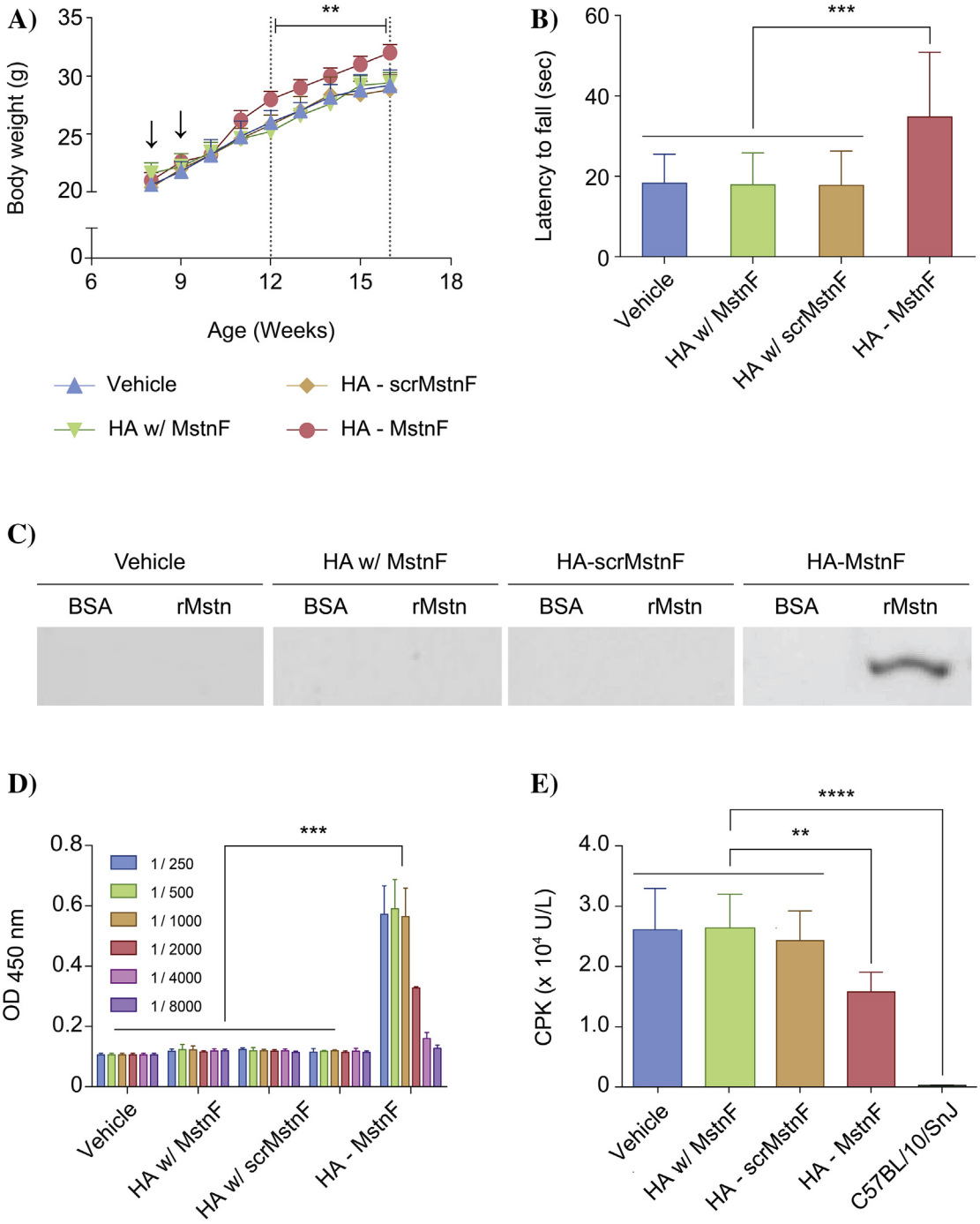

Fig. 5. Therapeutic effect of transdermal immunization with the control of vehicle, the mixture of HA and MstnF peptide, HA-scrambled MstnF conjugate, and HA-MstnF conjugate on (A) the body weight of *mdx* mice (small arrows - transdermal immunization), (B) the performance in the rotarod test of *mdx* mice, (C) the binding of antigen specific IgGs from *mdx* mice sera to myostatin, (D) the functional antibody titers with dilution by ELISA, and (E) the serum creatine phosphokinase (CPK) levels in *mdx* mice (n = 10).

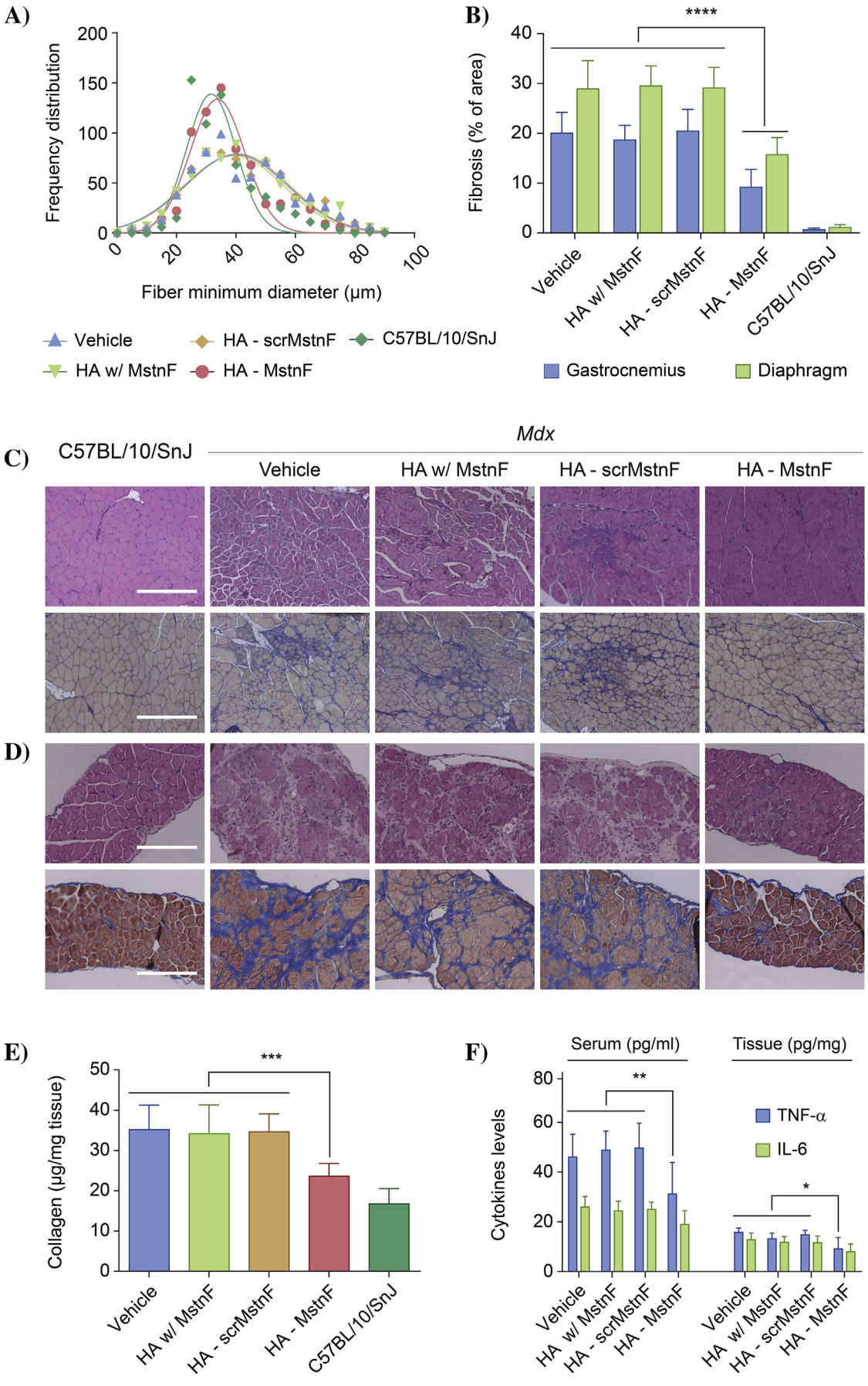
A)
Frequency distribution
Fiber minimum diameter (μm)
Vehicle
HA w/ MstnF
HA - scrMstnF
HA - MstnF
C57BL/10/SnJ
B)
Fibrosis (% of area)
****
Vehicle
HA w/ MstnF
HA - scrMstnF
HA - MstnF
C57BL/10/SnJ
Gastrocnemius
Diaphragm
C)
C57BL/10/SnJ
Mdx
Vehicle
HA w/ MstnF
HA - scrMstnF
HA - MstnF
D)
E)
Collagen (μg/mg tissue)
***
Vehicle
HA w/ MstnF
HA - scrMstnF
HA - MstnF
C57BL/10/SnJ
F)
Serum (pg/ml)
Tissue (pg/mg)
Cytokines levels
**
*
TNF-α
IL-6
Vehicle
HA w/ MstnF
HA - scrMstnF
HA - MstnF

cell culture supernatants were analyzed by ELISA for IL-1β, IL-6, IL-12, and TNF-α (Fig. 3). LPS (50 ng/mL) was used as a positive control in parallel to confirm the proinflammatory response of JAWS II cells to HA. The cytokine levels decreased with increasing molecular weight of HA (Fig. 3). The maximum cytokine release was observed by the stimulation with 5 kDa HA for all cytokines. The conjugation of HA (MW = 17 kDa) with MstnF resulted in only slight increase in the production of all proinflammatory cytokines by JAWS II cells. In contrast, the secretion of cytokines was negligible in cells treated with the vehicle (PBS) or the unconjugated MstnF peptide.

To expand our understating on the DC maturation by low MW HA, we also investigated the effect of hyaluronidase (0.01 unit/μg HA) on the production of cytokines (Fig. 3). Hyaluronidase can degrade HA, and is known to elicit a cutaneous inflammation and promote skin permeability [27]. In accordance, the secretion of proinflammatory cytokine levels significantly increased in the presence of hyaluronidase for various MW HAs. The results might suggest that catabolic degradation of HA by the extracellular degrading enzyme and the ROS mediated cleavage caused a synergistic effect on the activation, maturation, and migration of APCs. The hyaluronidase of Hyal-2 on the cell membrane degrades high MW HAs to HA fragment with an intermediate MW around 20 kDa. Furthermore, β-D-glucuronidase and β-N-acetylhexosaminidase can degrade oligosaccharide fragments by removing nonreducing terminal sugars. In contrast, the treatment with hyaluronidase or peptide alone did not affect the cytokine production.

It is noteworthy that HA can bind with HA receptors through 3 carboxyl groups [15]. Accordingly, the degree of HA modification with ALD should be less than 25 mol% for facile interaction with HA receptors in the skin cells and tissues. At this condition, because HA with a MW of 5 kDa has theoretically only about 3 ALD functional groups per a single HA chain (MW of repeating disaccharide unit = 401 g/mol), it may not be suitable for the delivery of multiple epitope antigens and the induction of immune responses. On the basis of this aspect and the almost comparable adjuvant effect, HA with a MW of *ca.* 17 kDa was used for the following *in vivo* studies.

3.3. In vivo two-photon microscopy of transdermal HA-MstnF conjugate

As shown in Fig. 4A, *in vivo* two-photon microscopy clearly visualized the effective transdermal delivery of HA-MstnF conjugate labelled with FITC through stratum corneum, epidermis, and dermis. The second harmonic generation signals revealed the collagen structure in dermal layers. After treatment with MstnF-FITC, however, there was no obvious fluorescence signal in all intact skin layers except the outermost layer of stratum corneum. The volume rendering of serial sections showed the transdermal transport of HA-MstnF-FITC conjugate through all intact skin layers (Fig. 4B). *Ex vivo* confocal microscopy also clearly confirmed the effective transdermal delivery of HA-MstnF conjugate (Fig. S5).

Transdermal vaccine delivery is an attractive alternative to conventional vaccine delivery as it can directly target the epidermal LCs and stimulate the immune system in the skin. As shown in Fig. 4C, the binding of HA-MstnF conjugate to LCs was clearly visualized by confocal microscopy after labeling HA-MstnF conjugate with FITC and immnohistochemical (IHC) staining of langerin in LCs. The green fluorescence of HA-MstnF conjugate was exactly merged to the red fluorescence of langerin positive cells. LCs play an important role in the immunization process, which activate and produce a large number of cytokines modulating the immune response and expressing intracellular adhesion molecules for immune cell migrations [28]. All these results revealed that low MW HA might be used as a natural adjuvant, delivering antigenic peptides directly to epidermal LCs or dermal DCs likely via HA receptors or TLRs.

3.4. In vivo transdermal treatment of muscular dystrophy

The effect of HA-MstnF conjugate on the transdermal treatment of muscular dystrophy was investigated by the analysis of body weight change, grip strength in rotarod tests, myostatin antibody formation, and serum CPK activity [29]. Fig. 5A shows the weekly body weight of immunized mice from 8 weeks to 16 weeks of age. While the body weight of *mdx* mice in the control group was unaffected, animals treated with HA-MstnF conjugates showed significantly increased body weights between 12 and 16 weeks of age. Furthermore, functional gains by the transdermal immunization were assessed by the rotarod test. After treatment with HA-MstnF conjugate, the rotarod performance was greatly improved to the statistically significant level in *mdx* mice at 16 weeks of age compared with the control groups (Fig. 5B). Such gains might be in line with myostatin inhibition in *mdx* mice exposed to anti-myostatin antibodies [3].

The therapeutic effect was further supported by the Western blot analysis of serum antibody for the binding affinity of IgGs to the recombinant murine myostatin (Fig. 5C). The serum IgGs from control groups did not show any functional antibody against myostatin. However, sera from mice immunized with HA-MstnF conjugate showed the presence of the specific antibody against recombinant murine myostatin. In accordance with the results, functional antibody titers by ELISA in sera from mice immunized with HA-MstnF conjugate were significantly higher than those with the vehicle, the simple mixture of HA and MstnF, and HA-scrambled MstnF conjugate (Fig. 5D). The improvement in the pathological status of the musculature was ascertained by the analysis of serum CPK activity (Fig. 5E), commonly used to diagnose DMD patients [30]. Highly elevated serum CPK levels were consistently noted in all control *mdx* mice. In contrast, a significant decrease of serum CPK was observed in the *mdx* mice after transdermal immunization with HA-MstnF conjugates, suggesting a reduction in muscle degeneration. All these results clearly confirmed the facile but effective transdermal immunization of HA-MstnF conjugates for early therapeutic intervention in dystrophin-deficient laboratory animals.

3.5. Histological assessment of muscular dystrophy

To date it is well established that the inhibition of myostatin results in the promotion of muscle regeneration [31]. Hence, we quantified the minimum diameter of single myofiber in gastrocnemius muscles at 16 weeks of age. As shown in Fig. 6A, there were significant changes in myofiber diameter and size distribution between *mdx* mice treated with controls and HA-MstnF conjugate ($P < 0.0001$). The immunized mice had fibers with a uniform diameter distribution statistically similar to that of wild type C57BL/10/SnJ mice ($P = 0.1187$), whereas fiber diameters significantly increased in the control *mdx* mice. The absolute number of

Fig. 6. Histopathological effect of transdermal immunization with the control of vehicle, the mixture of HA and MstnF peptide, HA-scrambled MstnF conjugate, and HA-MstnF conjugate on (A) the minimum diameter distribution of gastrocnemius muscle fibers in *mdx* mice at the age of 16 weeks (15 random regions per group) and (B) the ratio of the fibrotic area to the total area in the gastrocnemius and diaphragm muscle (n = 5, 5 fields from 5 slides per mouse). Histological analysis of (C) gastrocnemius muscles and (D) diaphragm muscles in *mdx* mice after staining with (top) hematoxylin and eosin and (bottom) Masson's trichrome (scale bar = 200 μm). Effect of the transdermal immunization on (E) collagen contents and (F) inflammatory cytokine levels in gastrocnemius muscle of *mdx* mice at the age of 16 weeks (n = 7).

myofibers in fifteen microscopic fields of the control *mdx* mice at 200 × magnification significantly decreased in comparison to those from age-matched wild-type and *mdx* mice immunized with HA-MstnF conjugate (Fig. S6). In addition, intrinsic muscle abnormality was evidenced by the relatively round shape with increased space between fibers, and the co-presence of both small and large fibers. The results might be ascribed to the compensatory muscle hypertrophy of hind limb muscles in the control *mdx* mice. Unlike in humans with DMD, the compensatory hypertrophy might result from the maintenance of a regenerative process in the *mdx* mice [32].

A striking feature of *mdx* muscle is the morphological cellular alternation by degeneration and hastened incomplete regeneration. Histological analysis of sectioned gastrocnemius muscles revealed gross abnormalities including extensive fibrosis and degeneration (Fig. 6B and C). However, *mdx* mice treated with HA-MstnF conjugates showed that morphological abnormalities were significantly reduced in the histological features, indicating the markedly decreased degeneration of myofibers and the subsequently reduced muscle fibrosis in *mdx* mice. *Mdx* mice have progressive muscle pathology, leading to the widespread accumulation of fibrous connective tissues [33]. The excessive accumulation of ECM causes the isolation of myofibers from capillaries and other myocytes, resulting in reduced contractility and regeneration [34]. To visualize the fibrosis, mouse muscle samples were stained with Masson's trichrome (Fig. 6C, bottom). The foci of fibrosis were frequently detected in the control *mdx* mice, which reflected the progressive replacement of myofibers with connective tissues. However, *mdx* mice treated with HA-MstnF conjugates resulted in a reduction of muscle fibrosis (Fig. 6B and C).

Compared to other muscles in the *mdx* mice, the diaphragm showed the early signs of the pathology with measurable muscle degeneration and fibrosis [35]. In accordance with the results from skeletal muscles, muscle architecture of the *mdx* mice immunized with HA-MstnF conjugate appeared similar with that of wild-type in the diaphragms (Fig. 6D). Histological evaluation of diaphragm muscle from control *mdx* mice showed the significant fiber loss and degeneration at 16 weeks of age compared to those from age-matched wild-type and *mdx* mice immunized with HA-MstnF conjugate. The *mdx* mice treated with HA-MstnF conjugates exhibited less fiber loss and degeneration. The ratio of the fibrotic area over total area examined per field in the diaphragm was significantly low for the case of immunization with HA-MstnF conjugate (Fig. 6B and D).

In agreement with previous reports [1,2,36], the collagen deposition was significantly reduced and the muscle histopathology on the level of inflammatory cytokine was greatly improved (Fig. 6E and F). To investigate whether the improvement was dependent on the up-regulation of utrophin, we further analyzed utrophin expression in gastrocnemius muscles. Despite histopathological distinctions, utrophin expression did not reveal any substantial qualitative difference between *mdx* mice treated with controls and HA-MstnF conjugate (Fig. S7). All these results indicate that transdermal active immunization against myostatin can be a promising strategy to suppress and combat the progressive weakness and degeneration of skeletal muscles of *mdx* mice.

4. Conclusion

We successfully developed a facile transdermal vaccine delivery system using HA - antigenic peptide conjugate to target and activate APCs. Although the exact mechanism remains unsolved, HA can be a novel and effective means for topical delivery of antigens to elicit the host immune responses. To our knowledge, this is the first report on the noninvasive transdermal intervention of DMD. This proof of concept study confirms that antigenic peptides conjugated to HA can be applied as a self-adjuvanted transdermal vaccine for the early intervention of various diseases including DMD. Our facile transdermal immunization strategy using HA - antigenic peptide conjugate might contribute greatly to the design and development of new paradigm vaccines.

Acknowledgements

This research was supported by a grant of the Korean Health Technology R&D Project, Ministry of Health and Welfare, Korea (HI14C1658). This study was supported by the Bio & Medical Technology Development Program (No. 2012M3A9C6049791) through the National Research Foundation (NRF) of Korea grant funded by the MEST.

Appendix A. Supplementary data

Supplementary data related to this article can be found at http://dx.doi.org/10.1016/j.biomaterials.2015.12.007.

References

[1] S. Bogdanovich, T.O. Krag, E.R. Barton, L.D. Morris, L.A. Whittemore, R.S. Ahima, et al., Functional improvement of dystrophic muscle by myostatin blockade, Nature 420 (2002) 418–421.
[2] Z. Bo Li, J. Zhang, K.R. Wagner, Inhibition of myostatin reverses muscle fibrosis through apoptosis, J. Cell Sci. 125 (2012) 3957–3965.
[3] T. Zhang, H. Yang, R. Wang, K. Xu, Y. Xin, G. Ren, et al., Oral administration of myostatin-specific whole recombinant yeast Saccharomyces cerevisiae vaccine increases body weight and muscle composition in mice, Vaccine 29 (2011) 8412–8416.
[4] L. Tang, Z. Yan, Y. Wan, W. Han, Y. Zhang, Myostatin DNA vaccine increases skeletal muscle mass and endurance in mice, Muscle Nerve 36 (2007) 342–348.
[5] T.A. Waldmann, Immunotherapy: past, present and future, Nat. Med. 9 (2003) 269–277.
[6] R.A. Lake, B.W. Robinson, Immunotherapy and chemotherapy–a practical partnership, Nat. Rev. Cancer 5 (2005) 397–405.
[7] C. Firbas, B. Jilma, E. Tauber, V. Buerger, S. Jelovcan, K. Lingnau, et al., Immunogenicity and safety of a novel therapeutic hepatitis C virus (HCV) peptide vaccine: a randomized, placebo controlled trial for dose optimization in 128 healthy subjects, Vaccine 24 (2006) 4343–4353.
[8] M. Larche, D.C. Wraith, Peptide-based therapeutic vaccines for allergic and autoimmune diseases, Nat. Med. 11 (2005) S69–S76.
[9] D.C. Wraith, Therapeutic peptide vaccines for treatment of autoimmune diseases, Immunol. Lett. 122 (2009) 134–136.
[10] M. Vanneman, G. Dranoff, Combining immunotherapy and targeted therapies in cancer treatment, Nat. Rev. Cancer 12 (2012) 237–251.
[11] S. Mitragotri, Immunization without needles, Nat. Rev. Immunol. 5 (2005) 905–916.
[12] T.S. Kupper, R.C. Fuhlbrigge, Immune surveillance in the skin: mechanisms and clinical consequences, Nat. Rev. Immunol. 4 (2004) 211–222.
[13] M.R. Prausnitz, R. Langer, Transdermal drug delivery, Nat. Biotechnol. 26 (2008) 1261–1268.
[14] J.A. Yang, E.S. Kim, J.H. Kwon, H. Kim, J.H. Shin, S.H. Yun, et al., Transdermal delivery of hyaluronic acid - human growth hormone conjugate, Biomaterials 33 (2012) 5947–5954.
[15] E.J. Oh, K. Park, K.S. Kim, J. Kim, J.A. Yang, J.H. Kong, et al., Target specific and long acting delivery of protein, peptide, and nucleotide therapeutics using hyaluronic acid derivatives, J. Control. Release 141 (2010) 2–12.
[16] T.J. Brown, D. Alcorn, J.R. Fraser, Absorption of hyaluronan applied to the surface of intact skin, J. Invest. Dermatol 113 (1999) 740–746.
[17] H. Kono, K.L. Rock, How dying cells alert the immune system to danger, Nat. Rev. Immunol. 8 (2008) 279–289.
[18] A. Biragyn, P.A. Ruffini, C.A. Leifer, E. Klyushnenkova, A. Shakhov, O. Chertov, et al., Toll-like receptor 4-dependent activation of dendritic cells by beta-defensin 2, Science 298 (2002) 1025–1029.
[19] D. Jiang, J. Liang, P.W. Noble, Hyaluronan as an immune regulator in human diseases, Physiol. Rev. 91 (2011) 221–264.
[20] C. Termeer, F. Benedix, J. Sleeman, C. Fieber, U. Voith, T. Ahrens, et al., Oligosaccharides of Hyaluronan activate dendritic cells via toll-like receptor 4, J. Exp. Med. 195 (2002) 99–111.
[21] L. Alaniz, M. Rizzo, M.G. Garcia, F. Piccioni, J.B. Aquino, M. Malvicini, et al., Low molecular weight hyaluronan preconditioning of tumor-pulsed dendritic cells increases their migratory ability and induces immunity against murine colorectal carcinoma, Cancer Immunol. Immunother. 60 (2011) 1383–1395.
[22] G. Bulfield, W.G. Siller, P.A. Wight, K.J. Moore, X chromosome-linked muscular

dystrophy (mdx) in the mouse, Proc. Natl. Acad. Sci. U. S. A. 81 (1984) 1189–1192.
[23] K. Palucka, J. Banchereau, Cancer immunotherapy via dendritic cells, Nat. Rev. Cancer 12 (2012) 265–277.
[24] D. Saunders, K. Lucas, J. Ismaili, L. Wu, E. Maraskovsky, A. Dunn, et al., Dendritic cell development in culture from thymic precursor cells in the absence of granulocyte/macrophage colony-stimulating factor, J. Exp. Med. 184 (1996) 2185–2196.
[25] L. Delamarre, H. Holcombe, I. Mellman, Presentation of exogenous antigens on major histocompatibility complex (MHC) class I and MHC class II molecules is differentially regulated during dendritic cell maturation, J. Exp. Med. 198 (2003) 111–122.
[26] A.E. Morelli, A.F. Zahorchak, A.T. Larregina, B.L. Colvin, A.J. Logar, T. Takayama, et al., Cytokine production by mouse myeloid dendritic cells in relation to differentiation and terminal maturation induced by lipopolysaccharide or CD40 ligation, Blood 98 (2001) 1512–1523.
[27] M. Fronza, G.F. Caetano, M.N. Leite, C.S. Bitencourt, F.W. Paula-Silva, T.A. Andrade, et al., Hyaluronidase modulates inflammatory response and accelerates the cutaneous wound healing, PLoS One 9 (2014) e112297.
[28] F. Geissmann, Y. Lepelletier, S. Fraitag, J. Valladeau, C. Bodemer, M. Debre, et al., Differentiation of Langerhans cells in Langerhans cell histiocytosis, Blood 97 (2001) 1241–1248.
[29] C.F. Spurney, H. Gordish-Dressman, A.D. Guerron, A. Sali, G.S. Pandey, R. Rawat, et al., Preclinical drug trials in the mdx mouse: assessment of reliable and sensitive outcome measures, Muscle Nerve 39 (2009) 591–602.
[30] H.J. van Ruiten, V. Straub, K. Bushby, M. Guglieri, Improving recognition of Duchenne muscular dystrophy: a retrospective case note review, Arch. Dis. Child. 99 (2014) 1074–1077.
[31] L.A. Whittemore, K. Song, X. Li, J. Aghajanian, M. Davies, S. Girgenrath, et al., Inhibition of myostatin in adult mice increases skeletal muscle mass and strength, Biochem. Biophys. Res. Commun. 300 (2003) 965–971.
[32] C. Dellorusso, R.W. Crawford, J.S. Chamberlain, S.V. Brooks, Tibialis anterior muscles in mdx mice are highly susceptible to contraction-induced injury, J. Muscle Res. Cell Motil. 22 (2001) 467–475.
[33] S. Sarma, N. Li, R.J. van Oort, C. Reynolds, D.G. Skapura, X.H. Wehrens, Genetic inhibition of PKA phosphorylation of RyR2 prevents dystrophic cardiomyopathy, Proc. Natl. Acad. Sci. U. S. A. 107 (2010) 13165–13170.
[34] V. Malik, L.R. Rodino-Klapac, J.R. Mendell, Emerging drugs for Duchenne muscular dystrophy, Expert Opin. Emerg. Drugs 17 (2012) 261–277.
[35] H.H. Stedman, H.L. Sweeney, J.B. Shrager, H.C. Maguire, R.A. Panettieri, B. Petrof, et al., The mdx mouse diaphragm reproduces the degenerative changes of Duchenne muscular dystrophy, Nature 352 (1991) 536–539.
[36] L. Zhang, V. Rajan, E. Lin, Z. Hu, H.Q. Han, X. Zhou, et al., FASEB journal : official publication of the Federation of American Societies for Experimental Biology, FASEB J. 25 (2011) 1653–1663.